IODINE CHEMISTRY AND MITIGATION MECHANISMS

FIKS-CT1999-00008

ICHEMM Final Synthesis Report

S Dickinson (Coordinator), G M N Baston and H E Sims, AEA Technology plc, UK
F Funke, Framatome ANP GmbH, Germany
R Cripps, H Bruchertseifer, B Jäckel and S Güntay, Paul Scherrer Institut, Switzerland
H Glänneskog and J-O Liljenzin, Chalmers University of Technology, Sweden
L Cantrel and M P Kissane, Institute de Radioprotection et de Sûreté Nucléaire, France
E Krausmann, EC Joint Research Centre, The Netherlands
A Rydl, Nuclear Research Institute Rez, Czech Republic

Dissemination level :   PU: public

IODINE CHEMISTRY AND MITIGATION MECHANISMS

CO-ORDINATOR

Dr S Dickinson
AEA Technology plc
108/B44, Winfrith Technology Centre
Dorchester
Dorset DT2 8DH
UK
Tel: +44 1305 202855
Fax: +44 1305 202663

LIST OF PARTNERS

1. AEA Technology plc, Winfrith, United Kingdom
2. Framatome ANP GmbH, Erlangen, Germany
3. Paul Scherrer Institut, Switzerland
4. Chalmers University of Technology, Sweden
5. Institute de Radioprotection et de Sûreté Nucléaire, France
6. EC Joint Research Centre, The Netherlands
7. Nuclear Research Institute Rez, Czech Republic

CONTRACT No: FIKS-CT1999-00008

EC Contribution	521879 EUR
Partners contribution	665977 EUR
Starting date	1 February 2000
Duration	36 months

CONTENTS

TABLES

FIGURES

LIST OF ABBREVIATIONS AND SYMBOLS

AEAT	AEA Technology plc
IRSN	Institut de Radioprotection et de Sûreté Nucléaire
LWR	Light Water reactor
BWR	Boiling Water Reactor
PWR	Pressurised Water reactor
SB-OUT	steam line break outside the containment with a subsequent loss of the secondary heat removal
HPI	High-pressure injection
MSH	Main steam header
PORV	Pressure relief valve
LB LOCA	Large-break loss of coolant accident
SGTR	Steam generator tube rupture

EXECUTIVE SUMMARY

A shared-cost action on Iodine Chemistry and Mitigation Mechanisms (ICHEMM) has been undertaken as part of the 5th Euratom Framework Programme on Nuclear Fission. Organisations from seven countries have been involved in an integrated programme of experiments, analysis and code development with the following objectives:

i.   to provide new experimental data for use in formulating models for volatile iodine destruction or transmutation reactions which are not routinely included in severe accident iodine chemistry codes;

ii.   to investigate other possible mitigation mechanisms or accident management measures to favour the conversion of volatile iodine species to non-volatile forms under severe accident conditions;

iii.   to provide new experimental data on iodine behaviour under conditions specific to BWR containments under accident conditions, and

iv.   to quantify the effects of the identified mitigation mechanisms on the predicted iodine source term for representative accident sequences.

New experimental measurements have been made of the rate of radiolytic decomposition of gaseous methyl iodide under a range of conditions (temperature, dose rate, humidity, atmosphere etc). A mechanistic model of the process has been developed to assist in interpreting the experiments and understanding the main reactions. An empirical model suitable for use in containment iodine chemistry codes has also been developed.

Experiments to measure the rate of reaction of gaseous I_2 with ozone in condensing conditions did not give definitive results due to problems with the analytical techniques that could not be surmounted. However, the limiting values obtained were consistent with measurements in non-condensing conditions. Rates of destruction of ozone at different surfaces were measured, showing that destruction is fastest at painted surfaces and at elevated temperatures. However, the reaction rate is not fast enough to significantly affect the kinetics of gaseous I_2 radiolytic destruction.

The effects of different chemical additives on the rate of destruction of irradiated aqueous CH_3I were experimentally studied with the aim of generating data for use in further development of procedures for accident management to retain organic iodine as far as possible in the reactor containment sump under severe accident conditions. At low temperatures ($\leq 50^0C$) and without additives, destruction by radiolysis is clearly dominant compared with hydrolysis. The pH effect does not appear significant with the range 5 – 9. Experiments with additives show that ammonium sulphide, sodium thiosulphate and especially Aliquat 336 and cysteamine are strong candidates for further investigations to ultimately improve accident management procedures.

The reaction of I_2 and CH_3I with reactive metal surfaces typically found in BWR containments (Al, Cu, Zn) has been studied. The reaction of gaseous I_2 with all three metals was fast; in the aqueous phase, significant absorption only occurs on Cu as the other two

metals cannot form an insoluble iodide product. Methyl iodide deposition onto the surfaces was much less efficient.

Five integral tests have been performed in the CAIMAN facility, extending the database on iodine volatility and organic iodide formation to higher temperature and dose rate, as well as condensing steam conditions. These tests showed that the predominant form of iodine in the gas phase was organic, mainly formed by reaction with dissolved organic materials in the sump.

A State-of-the-Art report on iodine chemistry and mitigation mechanisms was produced at the start of the project. During the course of the work, new models have been developed for various processes and these have been incorporated into containment chemistry modelling codes. An assessment has also been made of the relative importance of the different mechanisms for mitigating iodine volatility.

Plant calculations have been carried out to determine the effect of the new models on the iodine release in prototypic PWR and VVER sequences. This work has shown that the effect of the different mitigation mechanisms is dependent on the reactor type and sequence in question, with a greater impact being observed for the VVER sequence.

This programme has produced an extensive body of new data which can be used to validate iodine chemistry models under a range of conditions of relevance to severe reactor accidents. Various new models have also been developed during the course of the work that can be used in plant studies to improve the reliability of source-term assessments.

A   OBJECTIVES AND SCOPE

Reliable prediction of the radioactivity release which could occur as the result of a reactor accident is important for the design of accident management systems and strategies, as well as for setting regulatory requirements. This requires an adequate knowledge of the behaviour of the most radiologically important fission products. Plant assessments have shown that iodine contributes significantly to the source term for a range of accident scenarios. Iodine has a very complex chemistry which would determine its chemical form and, consequently, its volatility in the containment. At long times, gaseous iodine species may come to dominate the airborne iodine inventory in the containment, which is available for release to the environment through containment leakage or breach. The chemical form of the volatile iodine, specifically whether it is predominantly in an inorganic or organic form, will determine the efficacy of engineering safeguards such as containment sprays, pool scrubbers or containment venting filters, which can mitigate iodine release. The ability to predict the evolution of the airborne iodine speciation with increased confidence could therefore make an important contribution to the optimisation of management strategies. Furthermore, a sound understanding of the chemistry which controls the formation and destruction of volatile species is indispensable to the design of pre-installed mitigation measures and devices.

The chemistry of iodine under the conditions expected to prevail in the containment of a damaged LWR has been extensively studied in many laboratories throughout the world [1]. The main objective of these studies has generally been to understand and quantify the processes leading to the formation of volatile iodine, and most of the relevant processes are now adequately understood, in particular regarding the production of volatile I_2 from iodide dissolved in irradiated water. However, processes leading to the destruction of gaseous iodine, which could mitigate a possible release of iodine to the environment, are less well quantified. An improved knowledge of the destruction reaction rates will allow their potential importance to be assessed, in terms of both natural mitigation processes and potential accident management interventions.

Previous studies have tended to focus on conditions and phenomena occurring in large air-filled PWR containments. Relatively little work has been done under BWR containment conditions, although these constitute about a quarter of all operating power reactors. However, considerable differences exist between the conditions and materials present in the two types of containment, which will favour different chemical phenomena and could have a substantial effect on the iodine behaviour during a severe accident. Much remains to be learned and investigated in order to reach a level of understanding of iodine behaviour in BWR accident conditions similar to that in PWRs. In particular, there is a need for supplementary information on the effects of conditions or reactive components which are specific to these systems. Clarification of these issues will allow the evolution of gaseous iodine concentration and speciation within the reactor containment following an accident to be predicted with more confidence.

ICHEMM is an integrated programme of experiments and analysis aimed at increasing the knowledge base in the areas described above. The main technical objectives of the work programme were as follows:

i.   To provide new kinetic data for use in modelling the volatile iodine destruction or transmutation reactions which are not routinely included in severe accident iodine

chemistry modelling codes. This involved experimental measurements of the rate of molecular iodine destruction by ozone in the gas-phase, and of the rate of methyl iodide destruction under irradiation in the gaseous and aqueous phases. Integral tests were also undertaken to extend the database for model validation to high dose rate and elevated temperature.

ii.   To investigate other possible mitigation mechanisms or accident management measures to favour the conversion of volatile iodine species to non-volatile forms under severe accident conditions. This involved experimental studies of the effects of candidate additive materials on iodine volatility.

iii.   To provide new experimental data on iodine behaviour under conditions specific to BWR containments under accident conditions.

iv.   To quantify the effects of the identified mitigation mechanisms on the predicted iodine source term for representative accident sequences. This included the development of kinetic models based on the results of the experimental programmes, incorporation into severe accident modelling codes and evaluation of the impact on the calculated source term for some prototypical accident sequences.

The project, which brings together the main European laboratories working in the iodine chemistry field, has provided new experimental data on iodine behaviour under conditions which have not previously been studied, but which are of direct relevance to severe accidents in both PWR and BWR systems. These data have been used in the development of new or improved generic models for inclusion in existing iodine chemistry codes. The impact of the results in terms of possible improvements to plant safety and SAM strategies has also been considered.

B   WORK PROGRAMME

B.1   Gaseous methyl iodide destruction (WP1)
The rate of destruction of gaseous CH_3I by irradiation was measured under a range of conditions relevant to reactor containments. These data were used in the development and validation of a chemical model which can be applied in the prediction of iodine volatility in containment.

B.2   Reaction of gaseous I_2 with ozone (WP2)
The objective of WP2 was to produce kinetic data on I_2 oxidation by ozone in condensing steam atmospheres to extend and validate existing kinetic model on radiation-induced oxidation of gas-phase I_2. This included measurements of the rate of destruction of ozone at different surfaces.

B.3   Decomposition of aqueous organic iodides (WP3)
The effect of different chemical additives on the rate of destruction of aqueous CH_3I by irradiation was measured, with the objective of developing an accident management procedure for the reduction of the volatile organoiodide in the containment atmosphere.

B.4 Interaction of iodine with reactive metals (WP4)

This work package comprised a study of the interaction of gaseous and aqueous iodine and organic iodides with some reactive metals found in large quantities in BWR containments, and the development of models to simulate these interactions.

B.5 Organic iodide production at high temperature and dose rate (WP5)

This work package comprised five integral tests in the CAIMAN facility at high dose rate and elevated temperature under near-saturated steam atmospheres. The results of these tests extend the database available for iodine chemistry model validation.

B.6 Assessment and model development (WP6)

The overall objective of WP6 was to quantify the importance of radio-chemical processes in the determination and mitigation of the iodine source term. This included the production of a State-of-the-Art report (SOAR) on iodine chemistry and related mitigation mechanisms, and development of new models based on the experimental data generated in the other work packages.

B.7 Source term calculations (WP7)

This work package assessed the impact of the new data, models and procedures developed in Work Packages WP1 to WP6 on the calculated iodine source term for representative accident sequences, using calculations of typical PWR and VVER sequences.

C WORK PERFORMED AND RESULTS

C.1 Gaseous methyl iodide destruction (WP1)

The objective of this work package was to provide new experimental data on the kinetics of gaseous CH_3I destruction under irradiation, and to apply these data in the development and validation of a chemical model.

C.1.1 <u>Experimental procedures</u>

The initial stage of the work was to develop a suitable irradiation vessel and procedures for loading, sampling and analysing the CH_3I gas. The vessel was designed to allow gas samples to be taken at different times during the irradiation. This was achieved by using a septum, although particular measures had to be taken in the design to isolate this from both the test gas and the irradiation field. Methyl iodide was introduced by injecting a small quantity (5 - 500 µl) of a dilute aqueous solution, which vaporised to give a gaseous CH_3I concentration of about 5×10^{-8} mol dm^{-3}. The vessel was then irradiated by a ^{60}Co source at a γ dose rate of about 500 Gy hr^{-1}, and samples were removed periodically for analysis of the CH_3I concentration by gas chromatography. About 70 experiments were conducted under the following ranges of conditions:

Initial CH_3I concentration	$10^{-8} – 10^{-5}$ mol dm^{-3}
Temperature	$20 – 80°C$
Atmosphere	Air, 1% O_2/N_2, O_2, N_2 and N_2O
Humidity	Dry and humid atmospheres, liquid water
Dose rates	$5.5 – 560$ Gy hr^{-1}
Vessel surface area/volume ratio	$0.7 – 3.8$ cm^{-1}

C.1.2   Experimental results

The experimental results are summarised in Table I, which shows the average first order rate constants obtained by fitting the measured CH_3I concentrations to the expression

$$[CH_3I]_D = [CH_3I]_0 \, e^{-kD}$$

where D is the total dose. The decomposition rate in air at 20°C and a dose rate of 560 Gy hr^{-1} is about 7 (eV cm^{-3})$^{-1}$ or 1.5×10^{-4} s^{-1} (kGy hr^{-1})$^{-1}$. This is consistent with the only other study in the literature, which was conducted in dry air at ambient temperature [2].

The current work shows that increasing the temperature to 80°C increases the decomposition rate by less than a factor of 2. Most of the tests were carried out at this higher temperature since the results were less scattered. This work has confirmed that the radiolytic decomposition of CH_3I in air follows first-order kinetics in at concentrations below 10^{-6} mol dm^{-3}, as shown in Figure 1. Adding a larger volume of water had no effect at 25°C but appeared to decrease the decomposition rate slightly at 80°C; this may be due to the increased steam concentration rather than the presence of liquid water *per se*. The decomposition rate decreased by about a factor of 3 when the dose rate was reduced from 1 to 0.1 kGy hr^{-1} suggesting a square-root dependence, but this did not extend to very low dose rates. Decreasing the surface area to volume ratio below ~ 1 cm^{-1} did not affect the decomposition rate, but increasing the ratio above this caused a decrease in the rate, which is consistent with the destruction of reactive radicals at surfaces. Ethyl iodide was found to decompose at the same rate as CH_3I, and it is expected that all volatile alkyl halides expected to be formed in the containment would show similar kinetics.

The only parameter found to have a significant impact on the CH_3I decomposition rate was the bulk gas composition in the vessel. The rate was slightly lower in a steam/O_2 atmosphere, but much faster in pure N_2. A few tests were done under a N_2O atmosphere in the hope of gaining mechanistic information, but this fundamentally changed the gas phase chemistry so the results were difficult to interpret. Of most relevance to BWR studies were the results in 1% O_2/N_2 which showed much faster decomposition than in air.

C.1.3   Mechanistic modelling

A mechanistic model has been developed to describe the radiolytic destruction of I_2 and CH_3I in steam/air atmospheres. The predictions of the model were used in the interpretation of data from the above experimental studies as well as earlier work on I_2 radiolytic oxidation [3]. The model indicated that the main reactions responsible for the radiolytic destruction of I_2 are with O and OH radicals. Various intermediate gaseous species are formed, the most abundant being HI and $IONO_2$ under the conditions of the experiments modelled. Formation of the final solid oxide products occurs via reactions involving the minor intermediate species IO, I_2O_2 and IO_2, and there is considerable uncertainty in some of the rates and mechanisms of these reactions. The model gives good agreement with experimental measurements of gaseous I_2 concentration during irradiation. However, there are no data on the evolution of the total gaseous concentration against which the model can be validated.

The model also gave quite good agreement with the new experimental data on CH_3I decomposition. The most important aspects of the observed behaviour, for example the first order decomposition except at high CH_3I concentrations, the low temperature dependence and the effects of different atmospheres, were reproduced by the calculations.

The model indicates that main reaction responsible for the radiolytic destruction of CH_3I in air, at least at moderate to high dose rates ($\geq$500 Gy hr^{-1}), is with the electron. Although this accounts for only about 50% of the observed decomposition, no other significant reactant could be identified from the available kinetic data. The change in dose rate dependence at low dose rate observed in the tests indicates that another reactant becomes important at low dose rate. It has not been possible to identify this species from the current work, but a number of candidates can be postulated, all of which would give a square root dependence of the decomposition on dose rate. At very low dose rates (<10 Gy hr^{-1}) there is another change in the dose rate dependence which is not understood.

Two possible mechanisms have been identified by which the decomposition rate could be reduced at increased humidity. One of these, involving reaction between CH_3I and the O_2^- ion, would only be important at very low water concentrations so is of no relevance to reactor safety studies. However, at high humidity, increasing the water concentration would increase the rate of the reaction between electrons and O_2 via a third-body effect. Because the competition for electrons between CH_3I and O_2 has a determining effect on the kinetics, high steam concentrations will lead to a decrease in the CH_3I decomposition rate. The same competitive mechanism is responsible for the strong increase in the decomposition rate observed at low O_2 concentrations, which was well reproduced by the mechanistic model. The upper limit of CH_3I concentration, above which first order kinetics no longer applies, is decreased at low O_2 concentration.

The agreement between the model and experimental measurements of CH_3I decomposition in pure N_2 or N_2O atmospheres was less good than in air or O_2/N_2 mixtures. This reflects the fact that the chemistry of the system is fundamentally different in the absence of oxygen. This is of less importance for reactor accident studies since, even in inerted BWR containments, the O_2 concentration in the atmosphere will be much higher than that of iodine.

An empirical model for CH_3I decomposition in O_2/N_2 atmospheres has been formulated based on the experimental data and the mechanistic model:

$$\frac{d[CH_3I]}{dt} / s^{-1} = (zD + yD^n)[CH_3I]$$

where D is the dose rate in kGy hr^{-1},

$$z = \left(5 \times 10^{-5} + \frac{4500}{(3 \times 10^{10} + 6.9 \times 10^{11} x(O_2) + 4.97 \times 10^{12} x(H_2O))[M]^2 x(O_2)}\right) \exp\left(3.823 - \frac{1120}{T / K}\right),$$

$y = 5 \times 10^{-5}$ and $n = 0.5$. $x(O_2)$, for example, indicates the mole fraction of the bulk gas species.

This model is applicable for dose rates above 5 Gy hr^{-1}, and for $[CH_3I] \leq 10^{-7} x(O_2)$ in dry atmospheres or $CH_3I \leq 10^{-6} x(O_2)$ in atmospheres containing >10% H_2O. Under these conditions the model predicts the decomposition rate within a factor of 4.

The iodine species formed by the decomposition of CH_3I have not been identified, but the model indicates that, at reactor-relevant concentrations, I_2 is not formed. For modelling purposes, it is suggested that an intermediate species is defined which will deposit rapidly on

surfaces and dissolve in water films, thereafter becoming subject to the usual reactions of iodine under irradiation.

C.2 Reaction of gaseous I_2 with ozone (WP2)

C.2.1   Introduction and objectives

Work package 2 addresses the influence of radiation on volatile inorganic iodine in the containment atmosphere.

The influence of radiation on molecular iodine (I_2) in the atmosphere is indirect, namely through the action of reactive species from the radiolysis of air and steam. Ozone (O_3) is considered to represent air radiolysis products which in turn can oxidise the I_2 into non-volatile iodine oxides such as I_2O_5 and I_4O_9. These reaction products can subsequently be dissolved in aqueous droplets (formation of iodate, IO_3^-) under condensing-steam conditions or settle down as aerosols. In both cases, radiolytic oxidation of molecular iodine transforms the volatile iodine species (I_2) into non-volatile forms and thus can influence the source term.

Models exist that cover parts of the phenomena occurring in irradiated air/steam atmospheres containing I_2. However, the effects of condensing steam conditions and the effect of containment surfaces on the radiolytic oxidation of gaseous I_2 are not taken into account as data are missing. The associated effects were considered to effectively influence the iodine behaviour. It is thus important to extend the models based on experimental data under such boundary conditions.

The objective of work package 2 of the ICHEMM project was therefore to measure the rate constants of the reaction of gaseous I_2 with O_3 in condensing steam conditions and the destruction of O_3 at surfaces, considering O_3 as a representative of the air radiolysis products. The data are analysed with the aim to extend the existing models.

C.2.2   Literature review

The initial stage of the WP2 work was to review the literature on the radiolytic oxidation of I_2 in the containment atmosphere (deliverable D2.1). It turned out that essentially two experimental projects had produced data so far. The kinetics of the direct reaction between I_2 and O_3 in the absence of steam [4], and the rate of depletion of gaseous I_2 in irradiated air and dry steam / air atmospheres had been measured [3]. Models had been derived from these data to predict the radiolytic oxidation of gaseous I_2. The empirical model consists of the direct reaction between I_2 and O_3 to produce iodine oxides controlled by temperature and reactant concentrations, as well as production and decomposition of O_3 controlled by dose rate and temperature. O_3 was considered to represent air radiolysis products. Mechanistic models consider a variety of short-lived, reactive air radiolysis products, and O_3 is only one of several I_2 oxidising species. All models suffer from the fact that important parts of the relevant containment conditions were not covered, namely (1) the condensing steam conditions, and (2) the reaction of surfaces with air radiolysis products. Containment surfaces tend to decrease the concentration of air radiolysis products, thereby indirectly decreasing rate and extent of the radiolytic oxidation of I_2. It was therefore concluded to experimentally study (1) the I_2/O_3 reaction in condensing steam conditions, and (2) the destruction of O_3 at painted surfaces and steel surfaces.

C.2.3 I_2/O_3 reaction in condensing steam conditions

A complex apparatus was constructed to measure the kinetics of the I_2/O_3 reaction in condensing steam conditions at 100°C and ambient pressure. It was based on passing gas flows of I_2, O_3 from an electric discharge system and steam through a reaction vessel (2.2 litre, about 30 s reaction time) and absorbing the reaction products into liquids that identify the incoming species. The iodine absorber was based on a two-phase system, to trap I_2 in the organic solvent and iodine oxides in the water. The O_3 absorber consisted of an iodide solution where I_3^- is produced by O_3. The analytical determinations were generally done spectrophotometrically. Pre-tests with the individual components I_2, O_3 and steam showed promising results. The desired boundary conditions could be achieved and maintained during the tests with a sufficient degree of reproducibility.

However, in the main tests with both reactants introduced into the reaction vessel at the same time, no residual I_2 could be detected in the iodine absorbers behind the reaction vessel, even after several changes of the chemical trapping system. The most probable explanation for not finding I_2 in these absorbers is an additional I_2 destruction by residual O_3 within these absorbers. Such a disturbing process was indeed reproduced in separate tests. Based on this hypothesis the true final I_2 concentrations behind the reaction vessel should be higher than the measured lower limits. The rate constants derived from a standard data analysis with the Vikis model for non-steam conditions are thus upper limits. These upper limits for the rate constants of the I_2/O_3 reaction in steam (with and without condensation on walls) are consistent with the known kinetics in non-steam conditions. Being only upper limits, they do however not represent a progress for an extension of the modelling on radiolytic I_2 oxidation.

Based on the experimental facts alone, the possibility cannot completely be ruled out that the I_2/O_3 reaction in steam could have been much faster than in dry air. This in turn would mean that the corresponding rate constants would have to be extremely fast and very much higher than in non-steam conditions. The current tests were not designed and thus not able to measure data suitable to conclude about these interpretations.

A conceivable way-out to overcome the experimental difficulties in measuring the final I_2 concentration associated with the liquid iodine absorbers in any future project could be the direct spectrophotometric measurement of the gaseous I_2. However, large optical thicknesses in the order of 100 m (multiple reflexion) would be necessary to determine I_2 concentrations down to 10^{-8} mol dm^{-3}. The associated development of an appropriate spectroscopic device was beyond the scope of the current project.

C.2.4 Destruction of O_3 at surfaces

The kinetics of the ozone destruction at Epoxy paints and stainless steel was measured by placing samples with appropriate surface types and sizes into glass flasks filled with O_3. Initial O_3 concentrations were about 1.5×10^{-4} mol dm^{-3}. The O_3 was passed from an electric discharge system through the reaction vessel until saturation. The steel was generally in the as-received form, except of some tests at 80°C using electropolished steel. Tests were done in the absence of steam, between 20°C and 130°C by placing samples with appropriate surface types and sizes into glass flasks filled with O_3. Initial O_3 concentrations were about 1.5×10^{-4} mol dm^{-3}. The O_3 was passed from an electric discharge system through the reaction vessel until saturation. The steel was generally in the as-received form; some tests at 80°C were also done using electropolished steel. Tests were done in the absence of steam, between 20°C and 130°C. After given times the residual O_3 concentrations were determined by

absorbing the O_3 into iodide solutions, thereby inducing the formation of I_3^- and enabling the spectrophotometric determination of the I_3^- as a measure of the O_3. A pseudo-first-order model could be applied to derive the rate constants from measured decreases of O_3 concentrations with time. The background of thermal O_3 decomposition and O_3 decomposition at the glass surface was measured independently and subtracted.

The rate constants of the O_3 destruction at painted surfaces and steel surfaces increase strongly with temperature, following the Arrhenius model (see Figure 2). Paint is faster in destroying O_3 than stainless steel by roughly one order of magnitude (Figure 3). The obtained rate constants are suitable for inclusion in codes modelling the radiolysis of air or the gaseous iodine chemistry. The Arrhenius parameters required for implementing ozone decomposition at paint and steel in codes are $k(25°C) = 5.47 \times 10^{-7}$ m s^{-1}, activation energy = 58.3 kJ mol^{-1} for Epoxy paint and $k(25°C) = 6.42 \times 10^{-8}$ m s^{-1}, activation energy = 56.2 kJ mol^{-1} for steel.

Example calculations with the empirical model, extended by the above O_3 destruction at paint and steel, on the evolution of O_3 show that painted surfaces and steel surfaces exhibit only a small effect on the O_3 concentration. Thus, the I_2/O_3 reaction is practically not influenced by the lowering of the O_3 due to the O_3 destruction at the paint.

C.3 Decomposition of aqueous organic iodides (WP3)
C.3.1 Introduction and objectives
The main objective of the PSI experiments was to generate data for further development of measures for accident management in order to retain iodine in the reactor containment sump under severe accident conditions by reducing iodine volatility either to a minimum or ideally, completely. Iodine is either dissolved or suspended in the sump by transfer of gas phase components (molecular iodine and its compounds) through the gas-water interface, by settlement of iodine-containing aerosols, by airborne species removal using containment sprays and by transfer of condensate films containing dissolved iodine deposits from surfaces.

Radiation chemistry modifies the initial iodine species distribution. Iodine reactions with painted surfaces in the gas or liquid phase or with organic impurities in sump are known routes for organic iodide generation. Methyl iodide is one of the most volatile iodine species. It is the main organoiodine according to many small- and large-scale tests even at high pH.

C.3.2 State of the art
Upon entry into the containment, many processes in the primary circuit will determine the iodine speciation. Therefore, the initial and boundary conditions for the containment iodine chemistry are not easily described. The radiation chemistry of iodine in the containment is complex, such that even after very many years of research, different opinions exist about the main source of iodine in containment atmosphere, or about mechanisms of organoiodine formation. In particular, the priority of gas/solid phase reactions in the containment atmosphere and liquid/solid phase reactions in the sump. Measures must be taken to lower the volatile iodine in the containment gas phase by transfer to and retention in the reactor sump to hinder revolatilisation. They should ultimately and irreversibly fix the iodine by waste management measures so that iodine is ideally in a form for long-time storage.

Currently there is no consensus on organoiodine formation processes to make an accurate description. Therefore, formation and release into the containment atmosphere might not be effectively prevented by thermal or radiolytic decomposition. In worse cases, e.g., in a

sparged sump due to core-concrete interaction, organic iodide may be driven into gas bubbles faster than the decomposition rate. Therefore, the decomposition processes should be investigated and improved towards quantitative destruction. This work focuses on the study of aqueous organoiodine decomposition under reactor containment conditions. Its formation is not considered. This is especially important for reactor types containing a significant reactor sump or water volume in the containment.

C.3.3   Experiments to investigate the decomposition of methyl iodide

C.3.3.1 Experimental approach:

Scoping experiments with methyl iodide aqueous solutions under near-accident relevant conditions were performed to obtain more information on the destruction characteristics. Labelled (^{131}I) methyl iodide was synthesized and used as a sensitive indicator to track the iodine speciation. Two irradiation sources were used: The radionuclide ^{188}Re in aqueous solution with characteristics similar to those of the fission product mixture and γ-irradiation (^{60}Co: 1.5 kGy hr^{-1}). The latter was used to capture the process requiring short irradiation times and fast analytical measurements immediately following the irradiation.

C.3.3.2 Decomposition of CH$_3$I by hydrolysis and radiolysis (Deliverable 3.1)

Objectives of the experiments were to compare experimental data with literature data on hydrolysis and radiolysis under the range of conditions in the experiments including temperatures at 22°C, 50°C and 70°C (see Figure 4). Within the chosen experimental periods, decomposition by hydrolysis at 20-70°C is low. In 6 days at 22°C about 4 %, after 1.5 hours at 50^{0}C and after 45 min. at 70°C about 0.4 % and 13% decomposition was measured respectively. CH$_3$I decomposition by water radiolysis products also takes place, i.e. with solvated electrons (e$^-$) and hydrogen atoms (H•). The decomposition was investigated in air-saturated solutions at pH 5 – 9 (boric acid/borate) using a CH$_3$I concentration range from 10^{-6} to 10^{-3} mol.dm^{-3}, temperatures of 22 – 70°C and doses of 0 to 3 kGy. Table III shows that the radiolytic decomposition of 4×10^{-5} mol.dm^{-3} CH$_3$I solutions at 20-50°C is higher than hydrolysis under the same conditions. However, the pH and temperature dependency is weak. The decomposition is also clearly dose dependant. At a dose of between 1.4 and 3.1 kGy, complete decomposition was observed. Using 1.3×10^{-6} mol.dm^{-3} concentrations, the decomposition is somewhat lower. Comparing the results of hydrolysis with radiolysis it can be shown, that at lower temperatures (<50°C) and depending on the dose, radiolytic decomposition is dominant. At higher temperatures, closer to anticipated accident conditions (>90°C), hydrolysis will become more significant. Consequently such additional experiments would be of interest.

C.3.3.3 Decomposition of CH$_3$I with additives (Deliverable 3.2)

Of great technical and safety interest is the search for sufficient irradiation-resistant additives (see [5] for an overview) to enable rapid and complete CH$_3$I decomposition in solution to effectively compete with its mass transfer to the gas phase. CH$_3$I decomposition occurs thermally and radiolytically. Table IV and Table V show the results of the additives studied to enhance decomposition by one or both ways. Iodide from decomposing CH$_3$I can be sorbed on anionic exchangers or by combination with certain metallic ions to prevent CH$_3$I reformation. Hence Aliquat 336, trioctylamine and silver cations were also investigated. Additives which showed the most promising results were ammonium sulphide, thiosulphate [6] and Aliquat 336.

C.3.3.4 Methyl iodide decomposition modelling

Experimental results without additives or either with thiosulphate or formate additives were compared with computer-generated predictions using the PSIodine mechanistic code [7] with added models. The tests without additives have been fairly well predicted, although the modelling is still being developed. A mass transfer model for CH_3I and I_2 between the gas and water phases has predicted an expected retarding effect on CH_3I decomposition. A first model to predict the reducing effect of carboxyl radical ions, generated from irradiated formate ions, was added to the code. Predictions confirm the experimental results, namely that very little enhancement of CH_3I decomposition occurs in air-saturated CH_3I solutions. Once the O_2 is depleted by sufficient dose or impurities (Fe^{3+}/Fe^{2+}), rapid CH_3I decomposition is then predicted. But formate will also inhibit iodide oxidation to I_2 which is a precursor to CH_3I formation. Additionally a model for thiosulphate was also included to predict nucleophilic CH_3I decomposition and radiolytic thiosulphate decomposition. The thiosulphate comparisons are satisfactory.

C.3.3.4 Conclusions

The best CH_3I decompositions were obtained with ammonium sulphide, sodium thiosulphate, both at pH 9 and 70^0C and with Aliquat 336 at pH 5 and 22^0C. They show a good potential for improving procedures for accident management to decompose and/or fix methyl iodide or its product (iodide) in sump solutions or suspensions. Future work should provide a detailed and extended study of the best additives concluded from these results (WP3) by investigation of temperature (especially at $\geq 90^0C$) and pH effects, study of reagent additive mixtures (synergic effects etc.) and simultaneous iodide fixation. The results could then be applied as a basis to propose severe accident measures (spray or containment venting filter and pH-control solutions) in combination with nuclear waste management.

C.4   Interaction of iodine with reactive metals (WP4)
C.4.1   Introduction and objectives
Work package 4 addresses the influence of some reactive metals found in large quantities in a BWR on iodine species in the containment atmosphere.

Large areas in a BWR are reactive metals. Many construction details in the reactor containment are made of aluminium or exist as galvanized steel surfaces, i.e. covered with zinc. Also, in case of a meltdown, much wiring containing copper below the reactor tank will melt and release copper aerosols into the containment air [8]. Aluminium, zinc and copper are all fairly reactive and will undergo reactions with iodine in the containment.

There exist no models for the influence of these metals on the concentration of iodine species in the reactor containment and the objective of this work was therefore to provide empirical data on the reaction kinetics for volatile iodine species with copper, zinc and aluminium under conditions existing in a typical BWR reactor. These conditions include small amounts of oxygen but large amounts of hydrogen and water vapour. The influences of temperature, pH, and humidity were examined.

The iodine concentration in the BWR containment in case of a melt down is expected to be $\sim 10^{-5}$ M calculated from fuel composition. All experiments with iodine and metals within this work package have been performed at iodine concentrations of this magnitude.

C.4.2   Experiments and apparatus construction

Four experimental series were performed; experiments with gaseous iodine and metals under humid conditions (1), experiments with iodine and metals under dry conditions (2), experiments with iodine and metals in water (3) and experiments with methyl iodide and metals under humid conditions (4).

The first action within WP4 was to construct an apparatus to be able to conduct experimental series (1) and (2), (see Figure 3). The apparatus is viewed as being constructed in three parts – vessel and pipes, a temperature box and a detector system. All vessels and pipes were made of glass to minimize sorption of iodine species on these surfaces. To simulate the conditions existing in a BWR during an accident, the oxygen concentration inside the apparatus was kept low by flushing nitrogen gas, the vessel was filled with water to create a humid atmosphere, and all volumes and areas were proportional to those in a common BWR. The iodine concentration in the aqueous and gas phase was measured using a radioactive tracer. The metal samples were placed in the gas phase. In order to study iodine reactions with metals at elevated temperatures the apparatus was enclosed in a temperature regulation box. For experimental series (1) and (2) described here the flow rate of the aqueous phase and gaseous phase were 4.8 $cm^3 \cdot s^{-1}$ and 2.10 $cm^3 \cdot s^{-1}$ respectively. Experimental series (3) and (4) were performed using the vessel only with no circulation of phases or on-line measurements. The metal areas were the same in all experiments (Al - 8.77 cm^2, Zn - 4.63 cm^2, Cu - 0.99 cm^2) and the metals were always in the as-received form.

C.4.3   Experiments

Experiments with gaseous iodine and metals under humid conditions were performed by filling the apparatus partly with water, partly with nitrogen and gaseous iodine. After about one hour, equilibrium of iodine concentration between aqueous and gaseous phases was established and the metal (Cu, Zn or Al) was introduced to the gaseous phase. The decrease of iodine concentration in the aqueous and gas phase was measured as a function of time. The decrease of gaseous iodine concentration could be divided into two parts (see Figure 4). The first part was a fast initial exponential decrease due to sorption on the bare metal surface (Cu) or the metal oxide surface (Zn, Al). The second part was a slower exponential decrease due to diffusion through a built-up metal iodide layer. The reaction rate coefficient for the initial sorption, k_{sorp}, and the reaction rate coefficient for the slower decrease due to diffusion, k_{diff}, were derived (see Table I) from an exponential fit of the following equations to the experimental data:

$$[I_2]_t = [I_2]_0 \cdot e^{-k \cdot \frac{2 \cdot A}{V} \cdot t} \quad \text{(Cu)} \tag{1}$$

$$[I_2]_t = [I_2]_0 \cdot e^{-k \cdot \frac{A}{V} \cdot t} \quad \text{(Zn)} \tag{2}$$

$$[I_2]_t = [I_2]_0 \cdot e^{-k \cdot \frac{A}{3 \cdot V} \cdot t} \quad \text{(Al)} \tag{3}$$

where k is k_{sorp} or k_{diff} depending on which slope was examined.

Experiments with iodine and metals under dry conditions were performed using the apparatus with no water present. Reproducible results were difficult to obtain as the calculated adsorption rates differed two orders of magnitude. This behaviour could not be explained from the experiments performed.

For the experiments with iodine and metals in water the vessel was filled with water, gaseous iodine was dissolved in the water and the metal samples were placed in the aqueous phase. The amount of adsorbed iodine on the metal surfaces was measured after removal of metal samples at different times (1 hr, 3 hr, 19 hr and 22 hr). Iodine was adsorbed continuously on copper during the whole experiment. After 22 hr, 2 % of the total iodine inventory had been adsorbed on the copper surface. The adsorption rate was highest during the first few hours and decreased later. Zinc and aluminium showed no continuous uptake of iodine from the water. Handbook of Chemistry and Physics gives following values for the solubility of metal iodides in water: $CuI - 8 \times 10^{-6}$ g/dm^3, $ZnI_2 - 4.32$ g/dm^3, $AlI_3 -$ "soluble". This confirms that only copper would be able to continuously adsorb iodine when placed in water.

Experiments with methyl iodide and metals under humid conditions were also performed using the vessel partly filled with water. Radiolabelled CH_3I was added to the water phase and, as soon as equilibrium between the aqueous and gas phase was established, the metal samples were introduced to the gaseous phase. Each experiment was performed with an initial gaseous methyl iodide concentration of about 11 mM, which might seem fairly high but experimental difficulties made experiments at lower concentrations impossible. The amount of adsorbed methyl iodide on the metal surfaces was measured after removal of metal samples at different times.

The experiments performed at 25°C showed a surface concentration of 10^{-4} mol·m^{-2} after a few hours, and this concentration did not to change over time. All metals showed this behaviour. The experiments performed at 50°C indicated a somewhat higher surface concentration, in some experiments as high as 10^{-2} mol·m^{-2}, but data were scattered and any change of surface concentration as a function of time could not be verified. For the experiments performed at 80°C, copper showed a different behaviour compared to zinc and aluminium. The surface concentration of methyl iodide on copper increased with time as seen in Figure 5. The surface concentration increased over time and could be exponentially fitted to the expression $[S]_t = [S]_0 e^{-kt}$, where $[S]_t$ is the surface concentration in mol·m^{-2} at time t, $[S]_0$ is the initial surface concentration in mol·m^{-2}, t is the time and k is the first order surface adsorption coefficient in hr^{-1}. For copper experiments at 80°C k was calculated to 0.13 hr^{-1}. Zinc and aluminium did not show this behaviour. The surface concentration was generally higher at 80°C than at lower temperatures but no increasing adsorption with time could be seen.

C.5   Organic iodide production at high temperature and dose rate (WP5)
WP5 comprises five integral tests in the CAIMAN facility at high dose rate and elevated temperature under near-saturated steam atmospheres. The tests are summarised in Table VI. The results of these tests extend the database available for iodine chemistry model validation, particularly concerning iodine volatility and RI formation at high temperature and dose rate. The main results of each test are summarised in the following sections. Further and complete information can be found in the experimental reports [9].

C.5.1   Description of the CAIMAN facility
The schematic diagram of the facility is shown in Figure 8. The initial iodide concentration in the sump all the tests was 4×10^{-5} mol dm^{-3} labelled with [131]I. The radiation field was generated by a ^{60}Co source immersed in the sump. The gas phase was sampled

during the test using the Maypack device; I_2 and organic iodide (RI) concentrations are respectively trapped on knit mesh and charcoal filters and determined by γ-counting. The iodine activity on the deposition plates in the gas phase was also monitored on-line. Samples were taken periodically to determine the total organic carbon and some ion concentrations in the aqueous phase. At the end of the test, the γ-activities were counted on the different parts of the facility (immersed and non-immersed paints, steel walls, loop …) in order to establish a mass balance and an accurate determination of the distribution of iodine in the facility. Other measurements were made on-line throughout the test: the pH in the liquid circulation loop, the gas temperature at different levels, and the pressure.

C.5.2   CAIMAN 01

This test lasted around 70 hr. The gaseous molecular iodine concentration quickly reached a peak value of 1.8×10^{-10} mol dm^{-3}, but fell gradually to about 6×10^{-11} mol dm^{-3} over the next 50 hours. The gaseous organic iodide concentration increased gradually over the first 30 hours, to reach a maximum value of 5.5×10^{-10} mol dm^{-3}, but then decreased to about 3×10^{-10} mol dm^{-3} over the remainder of the test. The concentration of organic iodides in the gas phase was much greater than that of molecular iodine. A small fraction (≤1%) of iodine was trapped on the stainless steel walls of the vessel at the end of the test, and 1.3% of iodine was adsorbed onto the painted coupons in the gas phase.

C.5.3   CAIMAN 02

This test lasted 72 hr. The gaseous molecular iodine concentration quickly reached a peak value of 4×10^{-11} mol dm^{-3}, but fell gradually to about 10^{-11} mol dm^{-3} over the next few hours. The gaseous organic iodide concentration increased gradually over the first 30 hours, to a peak of about 2.0×10^{-10} mol dm^{-3}, but then slowly decreased. The concentration of organic iodides in the gas phase was again much greater than that of molecular iodine. The painted coupons in the sump were degraded to a large extent, so it was difficult to measure accurately the quantity of iodine deposited onto the surface. Nevertheless, this value is estimated to be about 5.5% of initial iodide inventory (i.i.i). The iodine trapped onto the gas painted coupons amounted to 1.9% i.i.i.

C.5.4   CAIMAN 03

This test lasted 162 hr, and was composed of three temperature stages. The first, at 130°C, lasted 43 hr and the second, at 110°C, 21 hr. During the last temperature stage, at 90°C, no measurements in the gas phase were carried out. The initial concentration was a bit lower than intended, only 2.9×10^{-5} mol dm^{-3}. Due to technical problems, the irradiation did not work between 2 hr and 18 hr. The rate of iodine adsorption onto painted surfaces in the gas phase appeared to be dependant on the temperature, increasing by a factor of 2 between 110°C and 130°C. The gaseous concentrations did not change strongly with the temperature. The average I_2 concentration at 110°C, 1.5×10^{-11} mol dm^{-3}, was approximately twice that at 130°C. This same trend was also observed for the RI concentration. At the end of the test, the iodine adsorbed onto the painted coupons was respectively to 4.1% and 8.0%/i.i.i in the gas and liquid phase.

C.5.5   CAIMAN 04

This test lasted 30 hr, and was performed under evaporating conditions with a condensation flow rate of about 0.07 g s^{-1}. Rapid mass transfer occurred in evaporating conditions, and a significant amount of iodine in the gas phase was measured after less than 2

hours. The mean molecular iodine concentration was 1.0×10^{-10} mol dm^{-3}. The first measurement of the organic iodide corresponds to 1.6×10^{-10}, before increasing to reach an average concentration of about 8×10^{-9} mol dm^{-3}. Both the molecular and organic iodide concentrations in the gas phase were increased compared with the tests under non-condensing conditions. The ratio of organic iodides to molecular iodine was higher than observed in the preceding tests, indicating that the production of RI was promoted by an increase of the mass transfer between sump and gas. At the end of the test, the iodine adsorbed onto the painted coupons rose respectively to 0.7% and 1.2%/i.i.i in the gas and liquid phase.

C.5.6 CAIMAN 05

This test lasted 140 hr. During the first part of the test (up to 70 hours), many problems with the irradiator device occurred; however, the correct irradiation conditions and sampling schedule was established for the second half of the test. The concentrations of organic and molecular iodine in the gas phase were about the same, in contrast with the earlier tests, probably because no painted coupon was present to trap the I_2. The gaseous fraction of molecular iodine is higher in comparison with the first three tests as no painted coupon is present in the gas and thus cannot trap I_2. The molecular iodine concentration reached a steady state concentration (3×10^{-10} mol dm^{-3}) and did not decrease as a function of time as observed in the preceding tests. The organic iodide concentration is similar at 5×10^{-10} mol dm^{-3}. In the liquid phase, 3.7%/i.i.i of iodine was adsorbed onto the painted coupons. A more elevated trapping occurred (5.7%/i.i.i) on the steel walls of the sump.

C.5.7 Interpretation of the CAIMAN tests with IODE5.1 code

The analysis of these tests has been performed with the IODE module included in ASTEC v1 [10]. This included the new aqueous RI formation model [11], described in Section C.6.2. A set of common parameters was defined (see Table VII). The desorption rate was taken as 10^{-4} s^{-1} for dry paint and a much lower value of 10^{-6} s^{-1} for wet paint at all temperatures. The overall mass transfer coefficient was set to 5.0×10^{-5} m s^{-1} for I_2 and 7.0×10^{-5} m s^{-1} for CH_3I. The difference is due to the fact that the diffusion coefficient of CH_3I is higher than that of I_2.

A very good general agreement between experimental data and IODE 5.1 is obtained, except for $[I_2](g)$ which is always overestimated by roughly one order of magnitude. The modelling of organic release from the paints has to be refined, especially for the paints located in the gas phase, knowing that in the reactor case they are in large excess in comparison with the potentially immersed paints. In the CAIMAN experiments, the main source of organic iodides present in the gas phase mainly comes from the sump. It contributes to more than 90% to the total $[RI](g)$, the remaining part being produced from the iodine adsorbed onto painted plates in the gas phase. This proportion can change a lot according to the dose rate value in the gas. Taking into account the possible radiolytic oxidation of I_2 into iodine oxide could improve the molecular iodine production because the oxide products would probably be rapidly transferred to the sump, particularly under condensing conditions.

C.6 Assessment and model development (WP6)

C.6.1 State-of-the-art report

The state-of-the-art report on iodine chemistry and related mitigation mechanisms in the containment (Deliverable D6.1, Ref. [12]) provides a general overview of the most relevant reactions involving various iodine species under severe-accident conditions in the

containment atmosphere and sump. It summarises the state of knowledge on the underlying reaction mechanisms at the beginning of the ICHEMM project and evaluates severe-accident management strategies to mitigate the consequences of an accidental iodine release.

Accident-management intervention in containment water bodies primarily focuses on inhibiting the volatilisation of dissolved *molecular iodine* formed by the radiolytic oxidation of iodide ions. Control of the sump pH at alkaline values offers itself as a practical and efficient mitigation tool, both increasing the rate of iodine reduction and directly acting on the formation of the hydroxyl radical, prerequisite for the radiolytic oxidation of iodide ions.

The initial solution pH is subject to changes in the course of an accident, brought about by the formation of inorganic and organic acids. Consequently pH control has to be effected by introducing strong bases or buffering agents into the sump. Candidate substances that were found to fulfil these requirements are, for instance, tri-sodium phosphate and borate/boric acid.

Addition of hydroxylamine nitrate effectively reduces dissolved molecular iodine to non-volatile iodide ions even at very acidic pH values.

Management of volatile *organic iodine* in the liquid phase is effected via control of its precursor substance molecular iodine. Maintaining an alkaline pH should therefore impede the extensive formation of aqueous organic iodides by keeping the molecular-iodine concentration at a very low level.

The interaction of iodine with immersed reactive metal surfaces can also reduce the aqueous iodine inventory. While immersed stainless steel surfaces tend to convert the adsorbed molecular iodine back to iodide ions, zinc-primer coated surfaces efficiently adsorb and retain volatile iodine at high pH values of about 9 to 10 under aerobic conditions. Upon contact with bases zinc surfaces can produce hydrogen, which has to be taken into account when alkalising the sump as an iodine-mitigation measure.

Silver is another potential reaction partner for aqueous iodine, which mitigates a possible iodine release by retaining iodine in the sump as non-volatile silver iodide. The greatest impact of the silver-iodine reaction is expected for low pH values and the presence of excess silver.

The second approach to severe-accident management is direct interference with the gas-phase iodine chemistry by augmenting the removal of airborne iodine.

Gaseous iodine behaviour during a severe accident is influenced by the reaction of molecular iodine with products of air radiolysis, generating involatile iodine aerosols that dissolve upon contact with droplets or sump water. This mitigation technique has the drawback that it requires oxygen for ozone formation and it is therefore not practicable in inert BWR containments.

Of particular interest is the adsorption of gaseous iodine on stainless steel or painted surfaces in the reactor containment. Both surface types have large adsorption capacities for molecular iodine under dry conditions, immobilising iodine, however, only temporarily in the

presence of oxygen. Steam-condensing conditions are more efficient in reducing the airborne iodine fraction by promoting the conversion of volatile I_2 to non-volatile iodide ions.

The use of spray systems and filters has been recognised as the most straightforward procedure for mitigating the release or formation of volatile iodine species. For the removal of gaseous molecular iodine alkaline spray solutions are preferable to acidic ones. The elimination of organic iodides by sprays is generally slower.

C.6.2   Data analysis and model development

The ICHEMM programme has produced a large body of new experimental data of relevance for both PWR and BWR accident conditions. These data have been used for modelling iodine removal or transmutation processes not commonly included in iodine-chemistry codes (Deliverable D6.2, Ref [13]). Incorporation of these new or improved models into severe-accident iodine-chemistry codes will allow the iodine behaviour within a post-accident containment to be predicted with a higher accuracy. This will improve the confidence in the predicted iodine source term and contribute to the optimisation of accident-management strategies.

A mechanistic model has been developed to describe the radiolytic destruction of I_2 and CH_3I in steam/air atmospheres. The main reactions responsible for the radiolytic destruction of I_2 are with O and OH radicals. The radiolytic decomposition of CH_3I is not strongly temperature dependent, and it largely occurs by reaction with the electron at moderate to high dose rates (>500 Gy/hr). The destruction rate is therefore directly proportional to dose rate. At lower dose rates another reaction with an as yet unidentified species becomes dominant and the decomposition rate no longer falls linearly with dose rate. The radiolytic decomposition of CH_3I is predicted to be higher in the lower O_2 concentrations in inerted BWR containment, as observed. An empirical model for the radiolytic decomposition of CH_3I has been developed based on the experimental results but informed by the mechanistic modelling (see Section C.1.3). This gives the decomposition rate constant as a function of dose rate, temperature and atmospheric composition (O_2, N_2 and H_2O concentrations).

The kinetics of the radiation-induced I_2 oxidation in the gas phase was investigated for steam-condensing conditions at 100°C. The results are consistent with the known kinetics in non-steam conditions and upper limits for the rate constants have been derived. Tests investigating the O_3 decomposition at containment surfaces as a function of temperature indicate an increasing influence of the surface in the order electropolished steel < steel < paint. The O_3 decrease due to the reaction with paint or steel can be modelled using a simple first-order mechanism. A new model suitable for incorporation into an empirical code like IMPAIR was developed.

A mechanistic model for the radiolysis of CH_3I in the presence of sump additives has been developed. New reactions have been added to the PSIodine model, describing CH_3I radiolysis and formate and thiosulphate chemistry. Mass transfer of CH_3I and I_2 to the gas space was also modelled and this was found to have a retarding effect on the decomposition. The formate radical ion will decompose CH_3I, but also reacts with O_2 so the decomposition of CH_3I is greatly reduced in aerated solution.

Tests on the deposition of gaseous I_2 on Cu, Zn and Al surfaces in the presence of water at temperatures up to 70°C suggested that there were two rate constants associated with the

reaction, which could be identified with an initial, rapid sorption process followed by slower diffusion of I_2 through a product layer. Both rate constants increased with temperature but were largely independent of the substrate metal. The rate constants for the initial sorption process ranged from 6×10^{-4} to 3×10^{-3} m s^{-1} (25 – 70°C) and the rate constants for the slower diffusion were in the range 3×10^{-5} to 3×10^{-4} m s^{-1} (25 – 70°C). Preliminary results for the reaction of CH_3I with metal surfaces indicate that only a minor uptake could be observed at 25 and 50°C. The results were the same for zinc and aluminium at 70°C, but copper showed a continuous uptake of CH_3I at 70°C. The rate of uptake on copper at this temperature was determined as 3.6×10^{-5} s^{-1}.

A promising new model for the homogeneous, aqueous-phase production of organic iodides has been implemented in the semi-empirical IODE code [10]. This model is based on the dissolution of residual organic compounds (RH), solvents or other low-molecular-weight additives, from the paint with formation of RI due to radiolytic degradation of these dissolved organics and their reaction with aqueous-phase molecular iodine. Sources of RH are painted surfaces that are either immersed or upon which condensation is occurring.

The key processes of the organic-iodide model are described below:

- Dissolution of organic solvents (RH) from painted surfaces
  This is described by a first-order kinetic expression.

- Reaction of hydroxyl radicals with dissolved RH
  The reaction of hydroxyl radicals with dissolved RH leads to the formation of organic radicals (R$\cdot$), which then react with I_2 to form organic iodides following the reaction pathway:
  $$RH + \cdot OH \rightarrow R\cdot + \ldots$$
  No reaction of RH destruction has been considered even if some possible radiolysis reactions could lead to the final formation of CO_2.
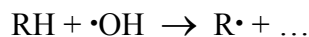
- Reaction of molecular iodine with organic radicals
  The organic radicals formed react with I_2 and O_2 following to the competitive reactions:
  $$R\cdot + I_2 \rightarrow RI + \ldots$$
  $$R\cdot + O_2 \rightarrow RO\cdot + \ldots$$
  All the rate laws and kinetic constants associated are provided in References [11] and [13].

The model has been tested and adjusted using data from a diversity of analytical tests. Furthermore, tests of the Caiman series have been analysed as part of the model validation process and good results were obtained.

C.6.3   Assessment of mitigation mechanisms

The different mechanisms for mitigating iodine release in a reactor accident have been assessed to give an indication of their relative importance. Although the assessment is mainly focussed on the release from containment following a LOCA in a PWR, the same principles can be applied to other sequences or reactor designs. The main findings of this analysis are as follows:

1. Homogeneous processes (hydrolysis, radiolysis) are important in reducing, and maintaining at a low level, the concentration of volatile species (I_2 and CH_3I) in containment water pools buffered to high pH (7-9).

2. Reaction of aqueous iodine with silver aerosol can result in the permanent immobilisation of iodine in an insoluble form under certain conditions. However, in high pH/high temperature conditions, silver iodide is not stable in a radiation field. The reaction of iodine with silver is therefore unlikely to bring any additional mitigation effect under conditions already optimised to minimise volatility. Silver iodide is also unstable in very acidic conditions (pH <3).

3. Reactions of aqueous species with other immersed surfaces (stainless steel, organic and zinc primer paints), whilst having a mitigative effect either through conversion of volatile to involatile species or by immobilisation of iodine, are not fast enough to have a significant impact on the iodine volatility.

4. Radiolytic oxidation of I_2 in the gas phase is a very fast process, and will generally be more important in lowering the gaseous I_2 concentration than reactions with surfaces and partition into water volumes. However, the products of this oxidation will initially be formed in the gas phase, and it is the behaviour of these species which will determine the evolution of the gaseous iodine activity. The products have not been identified for I_2 concentrations relevant to reactor accidents, but it is believed that they will be soluble and rapidly removed by dissolution in spray droplets or surface water films.

5. Radiolytic destruction of gaseous CH_3I, whilst slower than that of I_2, is of similar importance in being the dominant removal mechanism for this species. Whilst CH_3I destruction processes are much faster in water, the high volatility of this type of species means that only a small fraction of the total will be dissolved in a PWR containment.

6. In sequences where recirculating sprays are operational, radiolytic oxidation of I_2 and CH_3I in the gas phase reduces the steady state concentrations of these species by factors of about >2 and 10. The figure for I_2 reduction is a lower limit based on conservative assumptions about the oxidation kinetics; the true value could be substantially higher than this.

C.7   Source term calculations (WP7)
C.7.1   Introduction

The main objectives of WP7 were to assess the impact of the selected mechanisms studied within ICHEMM on calculated iodine source terms for VVER and PWR reactors. Among the mechanisms of the volatile iodine interactions studied in ICHEMM, the destruction processes of gaseous iodine species (CH_3I, I_2) in the containment atmosphere were of the primary interest for the computational simulations. The calculations have been performed using two empirical iodine-chemistry codes (or containment iodine codes): the modified French code IODE and the European code IMPAIR3. The work in WP7 started with selecting the severe accident scenarios, the course of which will be amenable to iodine mitigative measures. Representative PWR sequences had been defined previously in the 3rd RCA (Source Term) and the 4th Framework IC Programme, whereas the selection of the VVER sequences and their integral analyses with the MELCOR code were a substantial part of the presented work. Two principal mitigative mechanisms the effect of which was studied for both types of reactors (PWR and VVER) were radiolytic destruction of methyl iodide in

the containment atmosphere and radiolytic oxidation of molecular iodine by ozone in the atmosphere. For the IMPAIR3 PWR simulations there also has been studied the effect of the reaction of iodine with silver.

C.7.2   VVER iodine source term calculations using the modified IODE code

The SB-OUT sequence (steam line break outside the containment with a subsequent loss of the secondary heat removal) had been taken as a representative sequence for studying the volatile iodine behaviour at a severe accident in VVER-440/213. The sequence had been analysed with the MELCOR code (version 1.8.3) as a part of the WP7 work. In an integral simulation by MELCOR, all the boundary conditions for the subsequent containment iodine code runs are being defined. The sequence was further analysed with the IODE code for the volatile iodine formation and behaviour. Also, this sequence was later used for the evaluations of the effects of possible mitigative mechanisms studied within ICHEMM.

The accident starts with a break on a secondary steam line outside containment (main steam header rupture) and a subsequent loss of the secondary heat removal. For the sake of simplicity we assume that the whole secondary side will be isolated. High-pressure injection (HPI) is initiated immediately (from the MSH rupture signal) but the RCS pressure stays very high so the operator starts the bleed&feed by switching the containment sprays on (~1 hr) and opening the PORV (~1.5 hr). After opening the PORV, the signal for LPI is created and the accident would have been stopped if it were not for the common cause failure of both HP and LP pumps (at 2hr) some time later after the automatic switchover to recirculation. The containment sprays are working all the time[1]. The core melt accident initiated in such a way leads finally to vessel failure at low pressure (~8.5 hr) followed by an expulsion of the molten core to the cavity. Before the vessel failure, iodine in the form of CsI (and also other FPs) can escape from the RCS to the containment through the open PORV. The containment is isolated and the FPs are released to the environment through the normal leakage path. A significant release of iodine and other FP from damaged fuel is predicted to start at about 5h45min. MELCOR predicts that ~3.6 kg of iodine is released from fuel before the vessel failure (combining on release with Cs to form ~7.2 kg of CsI). About 1 kg of this iodine will get at that time to containment (the rest is retained in RCS). After vessel failure, almost all of the remaining iodine is released in reactor cavity at the high temperature core-concrete interaction (CCI) and via the restricted flowpath connecting cavity and the rest of the containment it gets to the containment atmosphere. The peak aerosol atmosphere concentrations in containment with maximum airborne CsI are reached at ~7hr (corresponding to ~0.7 kg of CsI in the atmosphere) and at ~11hr following CCI (~1.6 kg of CsI). All this mass is being slowly deposited in sump water as the aerosols fall out from the atmosphere. After 1 day, the amount of iodine in SG compartments (main containment volume with sump) is ~2.75 kg. Almost all of this iodine is dissolved in sump where there is about 650 m^3 of water.

---

[1] VVER-440/213 containments usually have some non-negligible operational (normal) leakage (can be up to 10% volumetric per day) and the FP release at an accident could be significant even for an intact containment. Releases of volatile matter to the environment could be non-negligible even with working containment sprays. This was the reason for considering the sequences with working sprays (in the Accident Progression Event Tree of the PSA Level 2) up to the evaluation of the source term to the environment. For the sequence under consideration, SB-OUT with sprays, the FP releases to the environment were also relatively high.

At the time when the first CsI gets to sump water (5 hr into the accident), the calculation of the iodine behaviour with the IODE code will start. Such a calculation yields a fraction of the total containment iodine which is in volatile form (I_2, organic iodides) in the containment atmosphere. This iodine, together with the airborne CsI mass (CsI carried on aerosols or sometime even in a vapour form), could be potentially released to the environment. If the containment is intact, the release goes via normal leakage flowpath (represented in the MELCOR model by a single hole of an equivalent diameter in the main containment volume). The atmosphere flows, containment leak rate, temperatures and pressures are all defined by the MELCOR calculation.

C.7.2.1 Results of the base case IODE calculation

According to the modified IODE, the total amount of the volatile iodine in the gas phase after 120 hr of the SB-OUT is 1.6×10^{-9} mol dm^{-3}. This represents about 2 grams of all the FP iodine (all iodine isotopes). Organic iodides form absolute majority of the total volatile iodine in the atmosphere.

The total volatile iodine leak to the environment after 5 days is about 0.3 gram. The total iodine release to the environment at this accident would then be the sum of the volatile iodine release and the release of I as CsI on aerosols. For this particular sequence, the particulate matter (aerosol) release of iodine to the environment - as calculated by MELCOR - is comparable to the volatile iodine release because of the effect of sprays (which rapidly wash out the aerosols from the containment atmosphere). Generally, the calculated aerosol releases of iodine for the VVER-440/213 containment at an accident are much higher than the volatile iodine releases but, at the same time, they are often overpredicted because the integral codes usually do not treat properly the containment leak path retention for aerosols.

C.7.2.2 Modelling of the mitigative mechanisms in the VVER simulations

The results of the base case SB-OUT scenario have been compared with simulations which involved the use of the AEA model of methyl iodide, CH_3I, destruction in the containment atmosphere and with calculations using the Framatome ANP model on the radiolytic oxidation of gaseous I_2. The results for the comparison were presented in [14] as volatile iodine species concentrations in the containment atmosphere and the total volatile iodine leak to the environment. These preliminary results of the VVER SB-OUT sequence simulation show that the first mechanism, CH_3I destruction in containment atmosphere, could have some effect on iodine release to the environment. This mechanism could lower the total volatile iodine atmospheric concentration and such a way it could lower also the volatile iodine source term to the environment. However, this is heavily dependent on the way we model the process: products of the reaction could be either non-volatile (or part of them could be non-volatile) and as such could be driven to water films on containment surfaces or to sump. Or these products are just I_2 (this was assumed for the PWR source term calculations described in the second part of this report) and the resulting effect on iodine source term could be very different. From the experimental data, this problem has not been definitely resolved at this stage of work. For the study of this mechanism we also badly need a good estimate of the dose rates in containment atmosphere (main parameter in the description of the reaction kinetics). Before we have some decisive evidence of the nature of the reaction products, the predictions of the effect of this mechanism on iodine release to the environment will be very uncertain. The other mechanism, the radiolytic oxidation of I_2 by ozone, did not significantly influence the total volatile iodine concentration in atmosphere in our

calculations. Thus, volatile iodine source term to the environment should not be lower due to this reaction. The formation of non-volatile iodine oxides in this reaction could even add to the total (volatile + non-volatile) iodine release in the IODE simulations. This is, however, rather a drawback of the modelling by a stand-alone code than a real effect.

C.7.3 PWR source-term calculations using the IMPAIR3 computer code

In this exercise, selected iodine mitigation models developed as part of the ICHEMM project were implemented into IMPAIR3 to assess the sensitivity of the iodine source term to the new models for representative PWR accident sequences. To this end revised models for the radiolytic oxidation of gaseous I_2 including the formation and decomposition of ozone, as well as for gaseous CH_3I destruction were incorporated in the code [13]). The IMPAIR3 multi-compartment calculations were based on PWR large-break LOCA and steam-generator tube rupture accident sequences owing to their importance in terms of risk to members of the public [15].

C.7.3.1 Large-break LOCA (LB LOCA) sequence

All non-chemistry data required to prepare the input deck were taken from Grindon *et al.* [16]) and Dickinson *et al.* [17]) and are based on MAAP predictions. The LB LOCA sequence was treated as a 2-compartment problem consisting of the containment (with a gas and a water phase) and the environment. Moreover, IMPAIR3 - like most other iodine chemistry codes - is limited to considering one water pool only, hence the separate pools in the reactor cavity and the lower compartment floor were approximated by a single water pool on the containment floor.

The timing and total mass of CsI and Ag aerosols released from the primary circuit was derived by a MAAP calculation and amounts to 12.1 kg of iodine and 360 kg of silver at *t*=8 hr, resulting in a Ag/I ratio of about 30. No gaseous iodine was predicted to be present in the containment initially. In the IMPAIR3 calculation CsI (I⁻) and Ag aerosols with a diameter of 5μ were assumed to enter the containment gas phase where they subsequently settled to the flooded containment floor. Following the failure of the reactor pressure vessel about 1 hour after the hot-leg break the fission-product discharge from the break in the primary circuit was assumed to stop at *t* > 1h.

The release of the airborne iodine species to the environment occurs via the design-basis leakage with a rate of 10^{-3} m^3/s. The same release rate was assumed for both aerosol and gaseous iodine species. This approach is conservative since the release rate for aerosols will most likely be lower due to particle deposition in the leak path.

The LB LOCA study was limited to the first 8 hours of the sequence due to the unavailability of the required thermalhydraulic parameters for longer times.

C.7.3.2 Results and conclusions for the LB LOCA calculations

Five calculations and accompanying sensitivity analyses have been performed to assess the impact of the new mitigation models on the iodine source term.

The performed sensitivity studies indicate that among the analysed mitigation mechanisms the silver-iodine reactions have the highest mitigation potential for gaseous iodine. To facilitate the assessment of the radiolytic CH_3I destruction and I_2 oxidation models

under conditions where the long-term iodine volatility is expected to be highest, all calculations testing these models were performed in the absence of silver.

Under the conditions of the analysed LB LOCA accident sequences the silver-iodine reaction has the greatest mitigation potential for gaseous iodine among the mitigation mechanisms analysed in the previous sections. The formation of stable silver iodide efficiently combats the volatilisation of iodine from the sump and consequently leads to very low gaseous iodine concentrations. The radiolytic decomposition of organic iodides in the gas phase also reduces the iodine source term although its mitigation potential appears to be negligible compared to that of the silver-iodine reaction. The role of the radiolytic oxidation of I_2 in mitigating the iodine source term is somewhat ambiguous. While the reaction reduces the I_2 fraction and thus the gaseous iodine release, the formation of iodine aerosols as a reaction product may in some cases counteract the desired mitigation effect.

The performed calculations indicate that during the initial, aerosol-dominated stage of the accident sequence the modelling of mitigation mechanisms that affect the gaseous iodine fraction has no major impact on the iodine source term. However, if molten core-concrete interaction is prevented, the total aerosol release is not likely to increase significantly compared to its value at 8 hr and the gaseous iodine fraction might become more important in the long term. Hence, there might be scope for iodine mitigation at the later stages of the accident sequence.

After settling of the airborne aerosols the iodine release to the environment will be dominated by gaseous iodine species. However, based on the very low gaseous iodine release predicted by IMPAIR3 for all studied boundary conditions, the *cumulative* release will still be dominated by aerosols at the time of complete containment depressurisation a couple of days after accident initiation[2].

C.7.3.3 Steam-generator tube rupture (SGTR) sequence

While the reactor is operating at full power a single steam-generator tube is assumed to sustain a double-ended guillotine rupture, which results in the discharge of primary coolant and associated fission products into the secondary side of the steam generator. There the increasing pressure may eventually exceed the set point of the pressure relief valve resulting in a release of fission products to the environment, which bypasses the containment. Assuming that the safety relief valve fails to close the release to the environment continues unabated, as does the discharge of primary coolant until the pressure in the secondary side is reduced to atmospheric pressure. Due to the unavailability of the emergency core cooling systems the core will uncover and eventually melt. After accumulation of sufficient corium the lower support plate will fail, releasing corium into the lower head of the reactor vessel. The vessel fails shortly thereafter, allowing all the corium to be deposited in the reactor cavity, where the water pool is boiled off and core-concrete interaction begins.

An analysis of the SGTR sequence using MAAP indicates that the reactor trips at 9 min into the accident, the steam generators are isolated by closure of the main steam isolation valves and the auxiliary feedwater supply to the steam generators is activated. At 2.6 hr

---

[2] It should be noted that the obtained results are based on the conservative but probably unrealistic assumption that both gaseous and aerosol iodine species are released with the same rate.

immediate shutdown is achieved. The core uncovers at 26.9 hr after opening of the safety relief valve and core melt commences at about 28.5 hr. After failure of the reactor vessel at 30.3 hr and the onset of core-concrete interaction at 34.2 hr the most likely failure mode for this sequence is basemat failure predicted to occur at 70h [16]).

The SGTR sequence was treated as a 2-compartment problem consisting of the steam generator (with a gas and a water phase) and the environment.

The timing and total mass of CsI and Ag aerosols released from the primary circuit to the secondary side was derived by a MAAP calculation and amounts to 215 g of iodine and 170 g of silver, resulting in a Ag/I ratio of < 1. The availability of the auxiliary feedwater guarantees that the break remains covered by water. Hence, in the IMPAIR calculation all the CsI (I^-) and Ag aerosols were assumed to enter the water phase of the steam generator. In contrast to the LB-LOCA sequence an aerosol diameter of 1μ has been used throughout the calculation.

The fission-product discharge from the submerged primary-circuit break was assumed to stop at about 33 hr shortly after the failure of the reactor vessel.

The release of the airborne iodine species to the environment occurs via the stuck-open safety relief valve. The same release rate was assumed for both aerosol and gaseous iodine species.

The SGTR study focuses on the analysis of the long-term behaviour of the iodine transferred to the steam generator and terminates at 72 hr after the initiating event.

C.7.3.4 Results and conclusions for the SGTR calculations
In the SGTR calculation the fission-product discharge from the primary circuit is assumed to be absorbed into the water phase of the steam generator. Iodine volatilisation occurs through mass transfer across the liquid-gas boundary or droplet carry-over due to drastic changes in the sump volume. Since the iodine fraction in the gas phase will predominantly be in gaseous and not aerosol form there is scope for iodine mitigation by action of the silver-iodine reactions or the radiolytic oxidation of molecular iodine.

The results of the SGTR source-term calculations confirm that the silver-iodide reaction has only a limited mitigation potential due to the low silver-iodine ratio in the sump. The radiolytic oxidation of I_2, on the other hand, does not appear to mitigate the gaseous iodine fraction at all but adds – albeit insignificantly – to the source term by producing iodine aerosols.

The SGTR calculations focused on the analysis of the long-term iodine behaviour under conditions where a non-negligible iodine volatilisation from the aqueous phase and a strong impact of the mitigation models was considered likely. However, due to mass-transfer limitations and the low dose rates in the steam generator the predicted iodine volatility and the release were very low. Interestingly, a crude comparison of the IMPAIR3 results and the predictions of other iodine-chemistry codes that had been applied to the same problem in an earlier project showed big differences in the released iodine fraction [16]). An analysis is called for to establish the reason for these differences. This is, however, beyond the scope of this project.

D CONCLUSIONS

A shared-cost action on Iodine Chemistry and Mitigation Mechanisms (ICHEMM) has been undertaken as part of the 5th Euratom Framework Programme on Nuclear Fission. Organisations from seven countries have been involved in an integrated programme of experiments, analysis and code development. New experimental data on the production, destruction and transmutation of volatile iodide have been provided. This has led to the development of models which have been incorporated in containment iodine chemistry modelling codes and applied in plant calculations of prototypical PWR and VVER scenarios. The efficiency of various additives which could be used to mitigate iodine release from containment water pools has also been investigated.

This programme has produced an extensive body of new data which can be used to validate iodine chemistry models under a range of conditions of relevance to severe reactor accidents. Various new models have also been developed during the course of the work that can be used in plant studies to improve the reliability of source-term assessments.

E REFERENCES

1   See various papers in:
     Proceedings of the specialists' workshop on iodine chemistry in reactor safety, September 1985, Harwell, UK, AERE-R 11974, 1986;
     Proceedings of the second CSNI workshop on iodine chemistry in reactor safety, Toronto, Canada, June 1988, CSNI-149, 1989;
     Proceedings of the third CSNI workshop on iodine chemistry in reactor safety, September 1991, Tokai-Mura, Japan, NEA/CSNI/R(91)15;
     Proceedings of the second CSNI workshop on the chemistry of iodine in reactor safety, June 1996, Wurenlingen, Switzerland, NEA/CSNI/R(96)6, 1996;
     Iodine aspects of severe accident management, Vantaa, Finland, May 1999, NEA/CSNI/R(99)7, 1999.

2   TANG, I N, and CASTLEMAN, A W Jr., Kinetics of γ-induced decomposition of methyl iodide in air, J Phys Chem, 74(22), 3933, 1970.

3   FUNKE, F, Literature review on the radiolytic oxidation of molecular iodine in the containment atmosphere, EC Project Report SAM-ICHEMM-D002, 2000.

4   VIKIS, A C and MACFARLANE, R, Reaction of iodine with ozone in the gas phase, J Phys Chem 89, 812 (1985).

5   PARSLEY L.F. , Chemical and physical properties of methyl iodide and its occurance under reactor accident conditions, ORNL-NSIC-82, 1971.

6   HASTY R.A., SUTTER S.L. , Kinetics of the reaction of methyl iodide with sulphite and thiosulphate ions in aqueous solution, Can. J. Chem. Vol. 47, pp4537-4541, 1969.

7   CRIPPS R., BUXTON G.V., SALMON G.A., PSIodine, an iodine mechanistic code, unpublished PSI report.

8   LILJENZIN, J O, Lindqvist, Influence Of Minor Materials On Iodine Behavior, Proc. Int. Cent. Heat Mass Transfer (Fission Prod. Transp. Processes React. Accid.) 30, 687-93 (1990).

9   SCHINDLER, P, Report on test CAIMAN 2001-01, SAM-ICHEMM-D007, 2002.
     SCHINDLER, P, Report on test CAIMAN 2001-02, SAM-ICHEMM-D008, 2002.
     SCHINDLER, P, Report on test CAIMAN 2001-03, SAM-ICHEMM-D015, 2002.
     SCHINDLER, P, Report on test CAIMAN 2001-04, SAM-ICHEMM-D018, 2003.
     SCHINDLER, P, Report on test CAIMAN 2001-05, SAM-ICHEMM-D019, 2003.

10   LIGER, K and CANTREL, L, IODE 5.1 description, Technical note IRSN/SEMAR 02/03, 2003.

11   TAYLOR, P, Transient formation of organic iodides: interpretation and modelling, Technical note IRSN/SEMAR 00/019, 2001.

12   KRAUSMANN, E, A state-of-the-art report on iodine chemistry and related mitigation mechanisms, EC Project Report SAM-ICHEMM-D003, EUR Report 19752 EN, 2001.

13   KRAUSMANN, E, Data analysis and modelling of iodine chemistry and mitigation mechanisms, EC Project Report SAM-ICHEMM-D010, 2002.

14   RYDL, A, and KRAUSMANN, E, Iodine Source Term Calculations, Shared-cost action document SAM-ICHEMM-D016, December 2002.

15   DUTTON, L M C, JONES, S H M, and EYINK, J, Reinforced concerted action on reactor safety, Source term project: Plant assessments, ST(93)-P35, Issue C Rev. 1, 1993.

16   GRINDON, E *et al.*, Iodine chemistry project, Task 3 – Source term evaluation, Shared-cost action document ST-IC/P(97)20, Rev. 1, 1998.

17   DICKINSON, S, and GRINDON, E, Minutes of meetings of the iodine chemistry project, Shared-cost action document ST-IC/M(97)07, 1997

Table I: Summary of rate constants for gaseous CH_3I destruction

T °C	D Gy hr^{-1}	Atmos-phere	[CH_3I] mol dm^{-3}	Water cm^{-3}	A/V	no of runs	k^a (eV cm^{-3})$^{-1}$	k^a s^{-1} (kGy hr^{-1})$^{-1}$
20	560	air	~5×10^{-8}	0.005	1.5	9	$6.1\pm3.7\times10^{-17}$	$1.3\pm0.8\times10^{-4}$
20	560	air	~5×10^{-8}	**0.5**	1.5	4	$7.7\pm2.5\times10^{-17}$	$1.6\pm0.5\times10^{-4}$
20	560	air	**10^{-7} C_2H_5**	**0.5**	1.5	2	$6.3\pm2.0\times10^{-17}$	$1.3\pm0.4\times10^{-4}$
20	**71**	air	~5×10^{-8}	0.5	1.5	2	$2.1\pm0.2\times10^{-16}$	$4.3\pm0.4\times10^{-4}$
20	**71**	air	~5×10^{-8}	0.5	**0.7**	2	$2.2\pm0.9\times10^{-16}$	$4.5\pm1.8\times10^{-4}$
20	**71**	air	~5×10^{-8}	0.5	**3.8**	1	8.4×10^{-17}	1.4×10^{-4}
20	**5.5**	air	2×10^{-7}	0.05	1.5	1	1.4×10^{-16}	2.9×10^{-4}
20	488	air	~2×10^{-7}	**"dry"**	1.5	2	$1.1\pm0.2\times10^{-16}$	$2.4\pm0.4\times10^{-4}$
20	488	air	**~10^{-5}**	**"dry"**	1.5	2	$2.0\pm0.2\times10^{-17}$	$4.0\pm0.5\times10^{-5}$
20	488	air	**8×10^{-5}**	**"dry"**	1.5	1	6.5×10^{-18}	1.4×10^{-5}
80	560	air	$1-55\times10^{-8}$	0.005	1.5	5	$1.3\pm0.1\times10^{-16}$	$2.2\pm0.2\times10^{-4}$
80	560	air	~2×10^{-7}	0.5	1.5	2	$7.3\pm0.7\times10^{-17}$	$1.3\pm0.1\times10^{-4}$
80	560	air	~4×10^{-7}	0.005	3.8	2	$5.9\pm0.9\times10^{-17}$	$1.0\pm0.2\times10^{-4}$
80	**58**	air	2×10^{-7}	0.05	1.5	1	8.6×10^{-17}	1.5×10^{-4}
20	560	**O_2**	~5×10^{-8}	0.005	1.5	3	$1.0\pm0.4\times10^{-16}$	$2.4\pm1.0\times10^{-4}$
20	**58**	**O_2**	10^{-7}	0.05	1.5	1	1.6×10^{-16}	3.7×10^{-4}
80	560	**O_2**	~8×10^{-8}	0.005	1.5	3	$8.4\pm1.3\times10^{-17}$	$1.6\pm0.4\times10^{-4}$
20	460	**1%O_2/N_2**	5×10^{-8}	0.05	1.5	1	9.3×10^{-16}	1.9×10^{-3}
20	460	**1%O_2/N_2**	**4×10^{-7}**	**"dry"**	1.5	1	2.7×10^{-16}	5.4×10^{-4}
20	**59**	**1%O_2/N_2**	4×10^{-8}	0.05	1.5	1	1.4×10^{-15}	2.7×10^{-3}
20	460	**N_2**	4×10^{-8}	0.05	1.5	1	1.7×10^{-15}	3.4×10^{-3}
20	**59**	**N_2**	~10^{-7}	0.05	1.5	3	$9.9\pm4.8\times10^{-16}$	$2.0\pm1.0\times10^{-3}$
20	480	**N_2O**	~2×10^{-7}	dry	1.5	2	$1.1\pm0.2\times10^{-16}$	$1.6\pm0.2\times10^{-4}$

a: uncertainties are 1σ

Table II: Reaction rate coefficients from the experiments with iodine and metals under humid conditions.

k_{sorp} is derived from an initial decrease of gaseous iodine concentration due to sorption on bare metal. k_{diff} is derived from a later slower decrease of gaseous iodine concentration due to diffusion of iodine species through a built-up layer of metal iodide.

metal	pH	temp (°C)	k_{sorp} (m/s)	k_{diff} (m/s)
Cu	7	25	8.62×10^{-4}	5.13×10^{-5}
Cu	7	50	9.74×10^{-4}	2.28×10^{-4}
Cu	7	70	1.90×10^{-3}	2.44×10^{-4}
Zn	7	25	6.88×10^{-4}	3.18×10^{-5}
Zn	7	50	1.05×10^{-3}	5.38×10^{-5}
Zn	7	70	2.21×10^{-3}	1.54×10^{-4}
Al	7	25	6.91×10^{-4}	3.69×10^{-5}
Al	7	50	1.08×10^{-3}	8.96×10^{-5}
Al	7	70	2.53×10^{-3}	2.48×10^{-4}

Table III. Radiolysis of CH$_3$I solutions without additives

Decomposition of CH$_3$I in buffer solution (boric acid/borate)

CH$_3$I [mol.dm^{-3}]	pH	Temp. ^{0}C	Dose [kGy]	Decomposition [%]
1.3.10^{-6}	5	22	1.4	83
1.3.10^{-6}	5	22	0.7	63
1.3.10^{-6}	9	22	0.8	70
1.3.10^{-6}	9	22	1.5	70
4.0.10^{-5}	5	22	3.1	95
4.0.10^{-5}	5	22	1.4	80
4.0.10^{-5}	9	22	1.4	83
4.0.10^{-5}	9	22	3.1	97
4.0.10^{-5}	5	50	0.7	63
4.0.10^{-5}	5	50	1.4	79
4.0.10^{-5}	9	50	0.7	66
4.0.10^{-5}	9	50	1.4	83

Table IV. Radiolysis of CH$_3$I solutions with additives

Decomposition of CH$_3$I in pH 9 buffer solution (boric acid/borate)

No. add	Additive / mol.dm^{-3}	Temp. ^{0}C	Dose [kGy]	Methyl iodide initial conc.	Methyl iodide remaining [%]
1	N$_2$H$_5$OH / 4.0E-03	22	0.38	4.0E-05	12
	ditto	22	0.00	ditto	99
	ditto	70	0.00	ditto	21
2	Cysteamine / 4.0E-03	22	0.38	4.0E-05	20
		22	0.00	ditto	16
3	(NH$_4$)$_2$S / 4.0E-03	22	0.38	4.0E-05	28
	ditto	22	0.00	ditto	47
	ditto	70	0.00	ditto	2
4	Trioctylamine / 3.6E-03	22	0.38	3.6E-05	48
	(TOA)	22	0.00	ditto	71
4a	Aliquat 336 / sat.soln.	22	0.38	3.6E-05	18
		22	0.00	ditto	75
5	Na$_2$S$_2$O$_3$ / 4.0E-03	22	0.38	4.0E-05	50
		22	0.00	ditto	74
		70	0.00	ditto	5

Table V. Radiolysis of CH₃I solutions with additives

Decomposition of methyl iodide in pH 5 buffer solution (boric acid/borate)

No. add	Additive / mol.dm⁻³	Temp. °C	Dose [kGy]	Methyl iodide initial [M]	Methyl iodide remaining [%]
1	Ag_2SO_4 / 4.0E-03	22	0.38	4.0E-05	49
		22	0.00	ditto	100
2	NaCOOH / 4.0E-02	22	0.38	4.0E-05	70
			0.00	ditto	97
3	TOA / 3.6E-03	22	0.38	3.6E-05	72
		22	0.00	ditto	94
3a	Aliquat 336 / sat.soln.	22	0.38	4.0E-05	2
		22	0.00	ditto	100
4	CuCNS / sat.soln.	22	0.38	4.0E-05	72
		22	0.00	ditto	100
5	$(NH_4)_2S$ / 4.0E-03	22	0.38	4.0E-05	75
		22	0.00	ditto	77
6	$Na_2S_2O_3$ / 4.0E-03	22	0.00	4.0E-05	86
7	Cl^- / 1.2E-02	22	1.40	1.0E-03	90
		22	0.00	1.0E-03	100
8	Formate / $CuSO_4$	50	0.38	4.0E-05	96
	4.0E-2 / 4.0E-3	50	0.00	ditto	99

Table VI. Matrix of the CAIMAN tests in WP5

Test	T_{liquid}			T_{gas}			pH	liquid paint	gas paint
01	110°C			110°C			5	no	yes
02	110°C			110°C			5	yes	yes
03	130°C	110°C	90°C	130°C	110°C	90°C	5	yes	yes
04	Sump evaporating						5	yes	yes
	117°C			90°C					
05	90°C			90°C			5	yes	no

Table VII. Adsorption coefficients for the different surfaces located either in gas or in liquid phase

|		k_{ads} dry paint	k_{ads} wet paint	k_{ads} dry steel	k_{ads} wet steel
		(m s⁻¹)			
Test 01	110°C	4.0 10⁻³	—	8.0 10⁻⁸	5.0 10⁻⁷
Test 02	110°C	4.0 10⁻³	1.0 10⁻⁴	1.0 10⁻⁶	1.0 10⁻⁶
Test 03	130°C	8.0 10⁻³	3.0 10⁻⁴	8.0 10⁻⁸	5.0 10⁻⁷
	110°C	4.0 10⁻³	1.0 10⁻⁴		
	90°C	1.0 10⁻³	5.0 10⁻⁵		
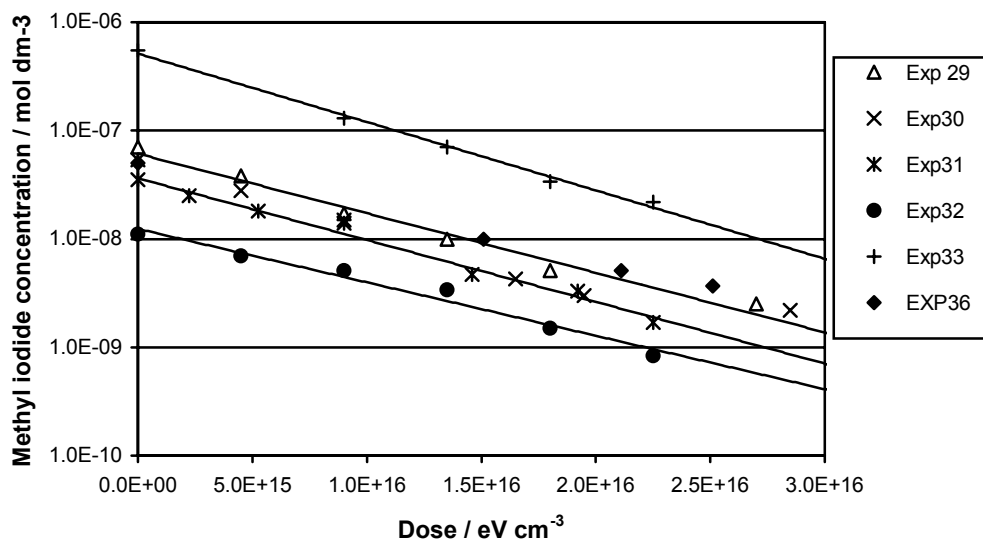
Figure 1. Decomposition of methyl iodide by γ irradiation in air at 80°C
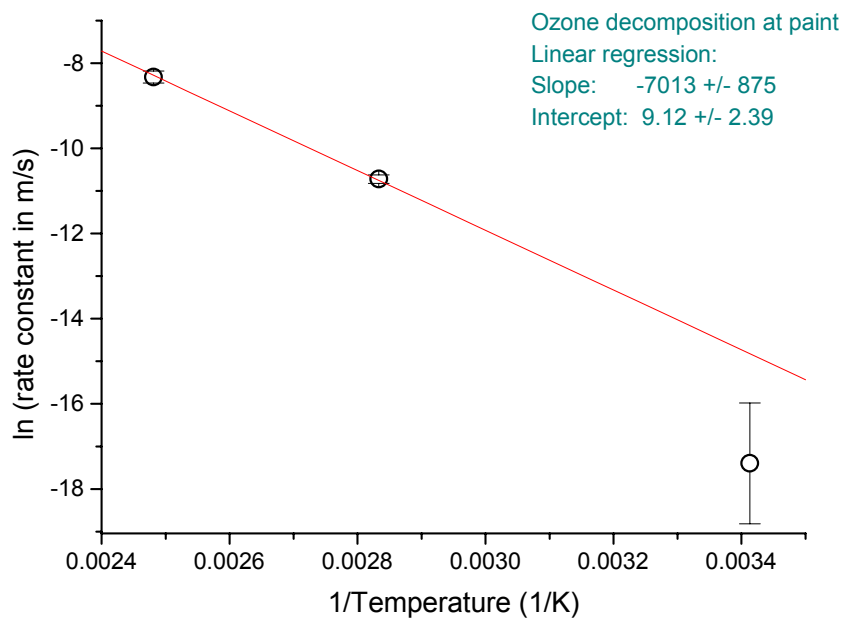
Figure 2. Arrhenius analysis of ozone decomposition at a painted surface
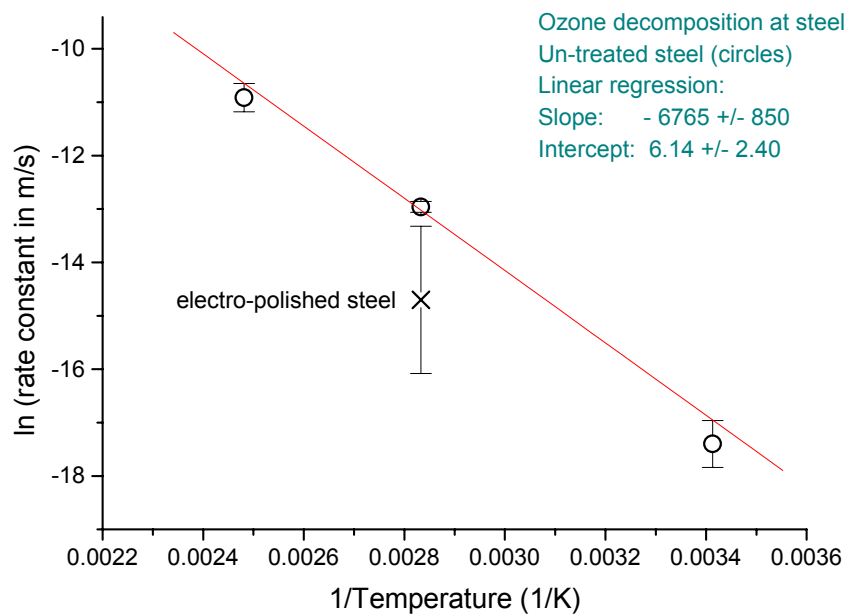
Figure 3. Arrhenius analysis of ozone decomposition at a steel surface
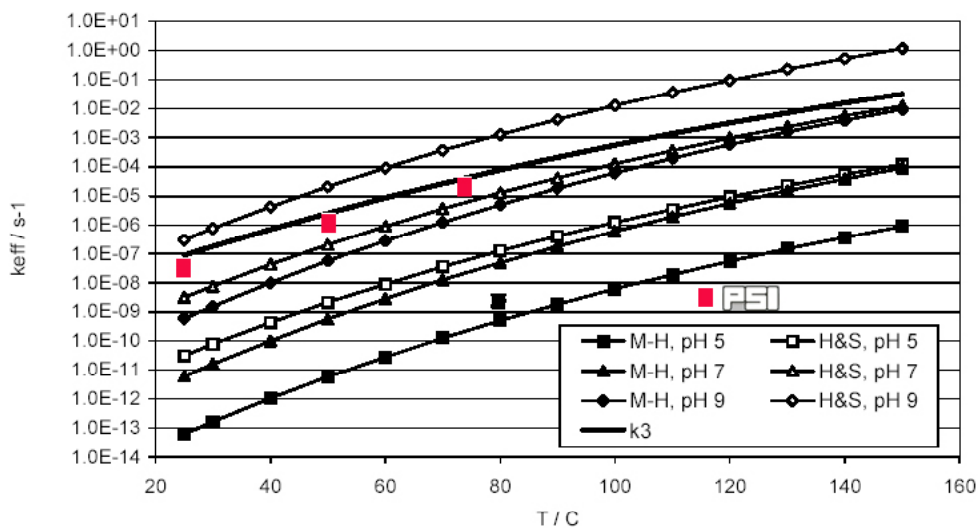
Rate constants for the hydrolysis of aqueous CH₃I
M-H: Moelwyn-Hughes, H&S: Hasty and Sutter, k₃: CH₃I + H₂O reaction

Figure 4. CH₃I hydrolysis: comparison of PSI data with literature data
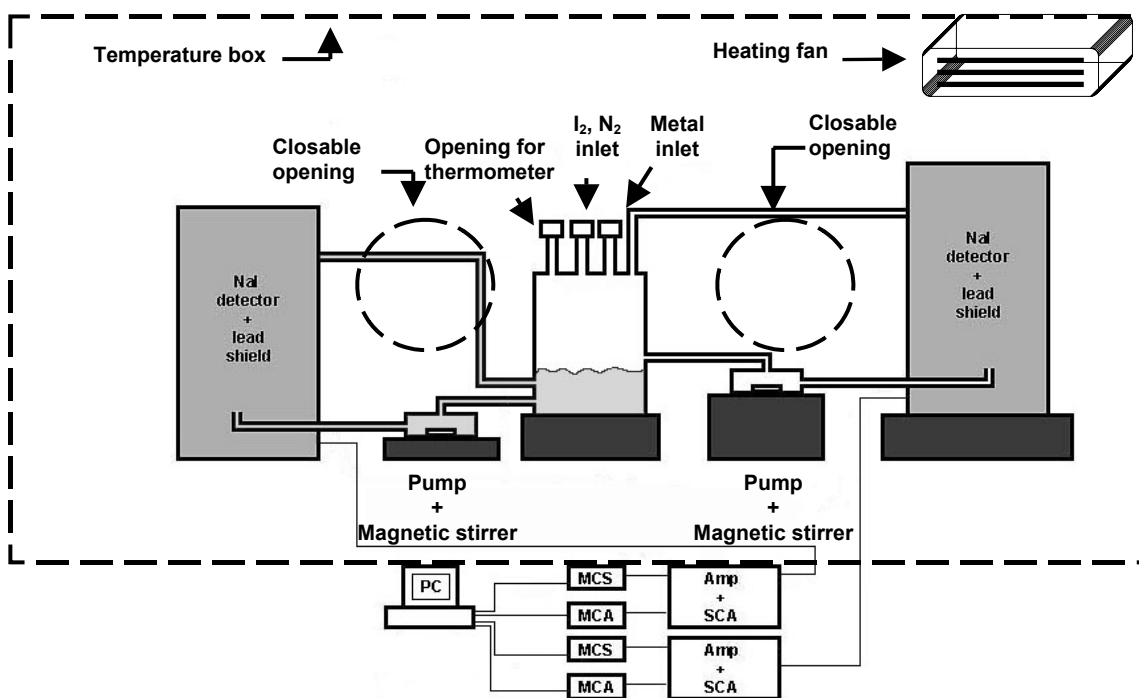
Figure 5. Sketch of the apparatus used for experiments with iodine and metals under humid conditions and for the experiments under dry conditions.
(The vessel used for the experiments with iodine and metals in water and the experiments with methyl iodide and metals under humid conditions is seen in the centre)
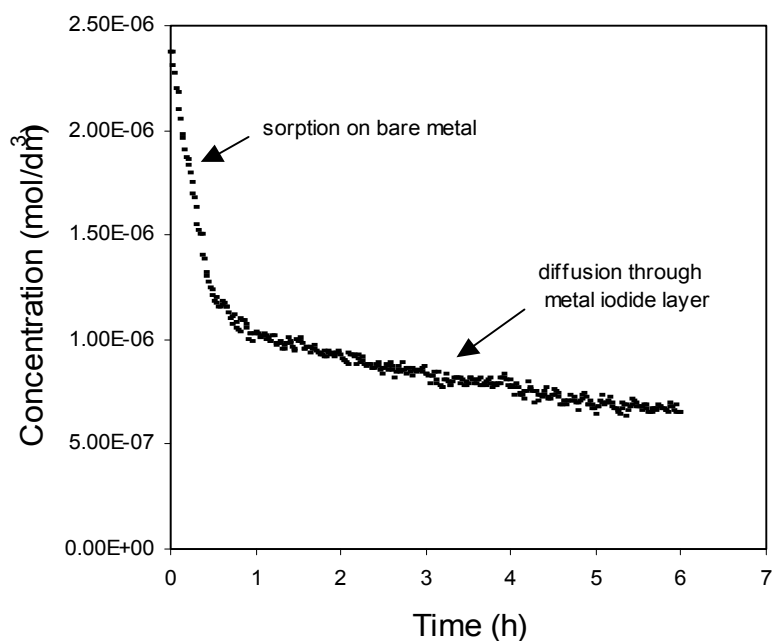

Figure 6. Decrease of gaseous iodine concentration for experiments with iodine and metals under humid conditions.
(Initially the decrease is fast due to sorption on bare metal. After some time the decrease rate is lowered due to diffusion through a built-up metal iodide layer.)
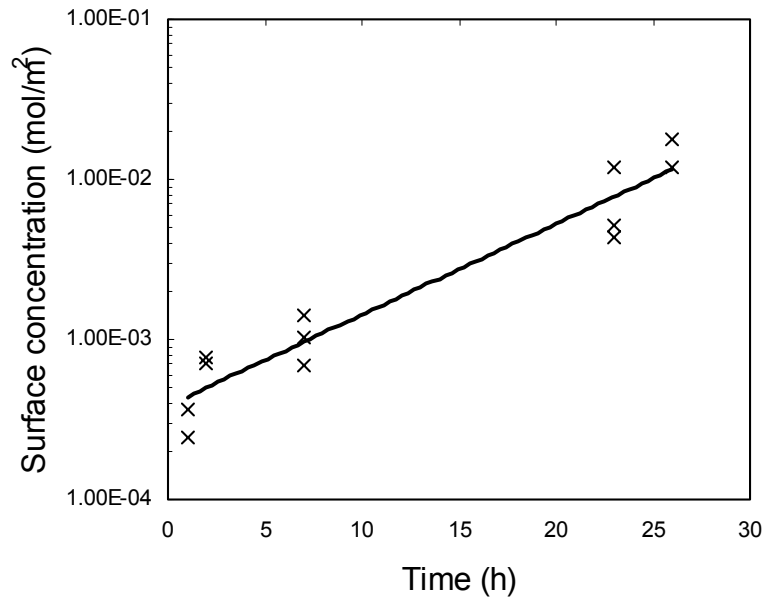
Figure 7. Methyl iodide surface concentration vs. time for copper placed in humid gaseous phase. Temperature = 80°C.
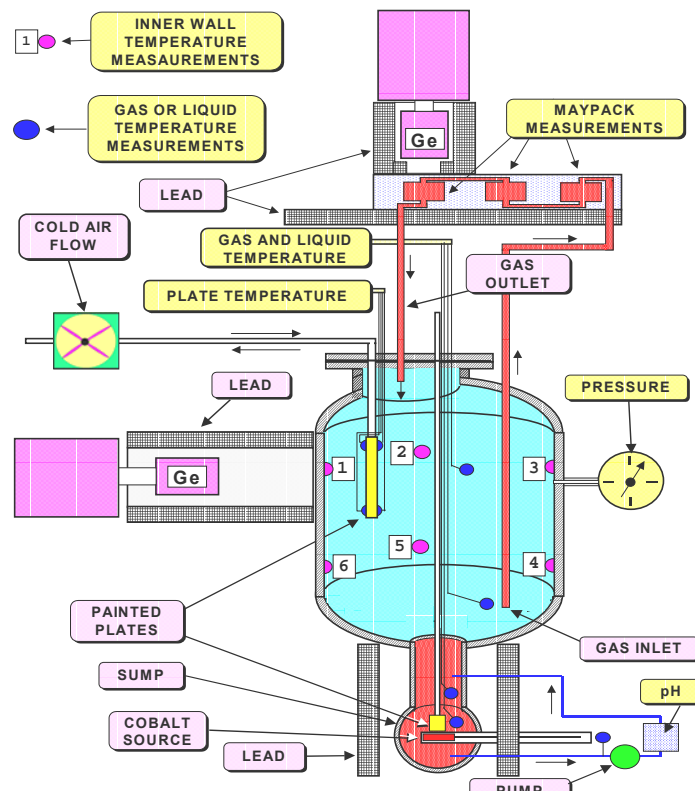

Figure 8. Schematic diagram of the CAIMAN facility with the associated instrumentation